Accepted Manuscript

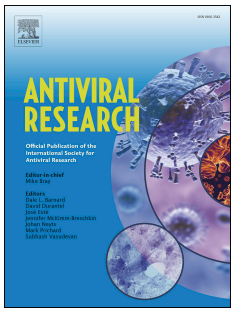

Structure-based drug design for envelope protein E2 uncovers a new class of bovine viral diarrhea inhibitors that block virus entry

María José Pascual, Fernando Merwaiss, Emilse Leal, María Eugenia Quintana, Alejandra V. Capozzo, Claudio N. Cavasotto, Mariela Bollini, Diego E. Alvarez

PII: S0166-3542(17)30598-3

DOI: 10.1016/j.antiviral.2017.10.010

Reference: AVR 4169

To appear in: *Antiviral Research*

Received Date: 23 August 2017

Revised Date: 9 October 2017

Accepted Date: 11 October 2017

Please cite this article as: Pascual, Marí.José., Merwaiss, F., Leal, E., Quintana, Marí.Eugenia., Capozzo, A.V., Cavasotto, C.N., Bollini, M., Alvarez, D.E., Structure-based drug design for envelope protein E2 uncovers a new class of bovine viral diarrhea inhibitors that block virus entry, *Antiviral Research* (2017), doi: 10.1016/j.antiviral.2017.10.010.

Structure-based drug design for envelope protein E2 uncovers a new class of bovine viral diarrhea inhibitors that block virus entry

María José Pascual[1], Fernando Merwaiss[1], Emilse Leal[2], María Eugenia Quintana[3], Alejandra V. Capozzo[3], Claudio N. Cavasotto[4], Mariela Bollini[2,§] and Diego E. Alvarez[1,#]

[1] Instituto de Investigaciones Biotecnológicas, CONICET, Universidad Nacional de San Martín, Argentina

[2] Centro de Investigaciones en Bionanociencias, CONICET, Argentina

[3] INTA-Instituto de Virología. Centro de Investigaciones en Ciencias Veterinarias y Agronómicas, Buenos Aires, Argentina

[4] Laboratory of Computational Chemistry and Drug Design, Instituto de Investigación en Biomedicina de Buenos Aires (IBioBA) – CONICET – Partner Institute of the Max Planck Society, Argentina

[#] Corresponding author. Instituto de Investigaciones Biotecnológicas, CONICET, Universidad Nacional de San Martín, San Martín (B1650HMR) Argentina. dalvarez@iibintech.com.ar

[§] Corresponding author. Centro de Investigaciones en Bionanociencias, CONICET, Buenos Aires (C1425FQD) Argentina. mariela.bollini@cibion.conicet.gov.ar

Abstract

Antiviral targeting of virus envelope proteins is an effective strategy for therapeutic intervention of viral infections. Here, we took a computer-guided approach with the aim of identifying new antivirals against the envelope protein E2 of bovine viral diarrhea virus (BVDV). BVDV is an enveloped virus with an RNA genome responsible for major economic losses of the cattle industry worldwide. Based on the crystal structure of the envelope protein E2, we defined a binding site at the interface of the two most distal domains from the virus membrane and pursued a hierarchical docking-based virtual screening search to identify small-molecule ligands of E2. Phenyl thiophene carboxamide derivative 12 (PTC12) emerged as a specific inhibitor of BVDV replication from *in vitro* antiviral activity screening of candidate molecules, displaying an IC_{50} of 0.30 µM against the reference NADL strain of the virus. Using reverse genetics we constructed a recombinant BVDV expressing GFP that served as a sensitive reporter for the study of the mechanism of action of antiviral compounds. Time of drug addition assays showed that PTC12 inhibited an early step of infection. The mechanism of action was further dissected to find that the compound specifically acted at the internalization step of virus entry. Interestingly, we demonstrated that similar to PTC12, the benzimidazole derivative 03 (BI03) selected in the virtual screen also inhibited internalization of BVDV. Furthermore, docking analysis of PTC12 and BI03 into the binding site revealed common interactions with amino acid residues in E2 suggesting that both compounds could share the same molecular target. In conclusion, starting from a targeted design strategy of antivirals against E2 we identified PTC12 as a potent inhibitor of BVDV entry. The compound can be valuable in the design of antiviral strategies in combination with already well-characterized polymerase inhibitors of BVDV.

Keywords: BVDV; pestivirus; docking; virtual screening; reporter virus; antivirals

1-Introduction

Bovine viral diarrhea virus (BVDV) together with classical swine fever virus (CSFV) and border disease virus (BDV) of sheep are pestiviruses in the family *Flaviviridae* of positive-strand RNA viruses. The family comprises human pathogens such as dengue virus, zika virus or tick-borne encephalitis virus that are flaviviruses transmitted by insect vectors, and hepatitis C virus that is a blood-borne virus and the only member of hepaciviruses (Lindenbach et al., 2007). Viruses in the *Flaviviridae* family differ in the organization of their genomes and the structure of the virus particle. In particular, the RNA genome of pestiviruses encodes a large polyprotein that is processed into individual viral proteins: N^{pro} -C-E^{rns} -E1-E2-p7-NS2-NS3-NS4A-NS4B-NS5A-NS5B (Collett et al., 1988). Pestivirus particles consist of a lipid bilayer with envelope glycoproteins E^{rns}, E1, and E2 surrounding the nucleocapsid, composed by the capsid protein C and the RNA genome (Callens et al., 2016).

BVDV infection is distributed worldwide resulting in major economic losses to the livestock industry. The virus is primarily a pathogen of cattle and the clinical manifestations are presented as acute infection, fetal infection, or mucosal disease (Lanyon et al., 2014). Based on genetic and antigenic differences, BVDV is segregated into genotypes 1 and 2. For each of these genotypes, cytopathic and non-cytopathic biotypes are distinguished according to the capacity of virus infection to induce cell death in culture (Ridpath, 2003). Non cytopathic (ncp) BVDV biotypes cause acute infections in adult animals and can be transmitted across the placenta to the fetus. Fetal infection is particularly relevant and it can lead to congenital malformations and abortion, or to the birth of persistently infected (PI) calves that spread and maintain the disease in cattle populations (Lanyon et al., 2014). Cytopathic (cp) BVDV biotypes arise in PI cattle from recombination events in the infecting ncpBVDV genome, and are associated with the development of fatal mucosal disease (Becher and Tautz, 2011).

Control and prevention of BVDV infection should combine systematic vaccination with detection and culling of persistently infected cattle from herds (Newcomer and Givens, 2013). However, immunization is complicated due to the wide antigenic diversity of the virus, and fails to target the emergence of persistently infected animals (Fulton et al., 2003; Newcomer et al., 2017). According to previous observations showing that antivirals provide immediate protection from viral challenge (Newcomer et al., 2012; Newcomer et al., 2013a), prophylactic treatment with antivirals provides an alternative for therapeutic intervention in outbreaks of BVDV.

To date, specific strategies to tackle BVDV replication with antiviral compounds were mostly targeted against the NS5B RNA-dependent RNA-polymerase (RdRp) and to a lesser extent against the NS3 helicase and serine protease (reviewed in (Newcomer and Givens, 2013)). As for other RNA viruses, the development of antiviral strategies for BVDV has encountered the rapid selection of resistant virus populations as a common pitfall. Therefore, the design of effective antiviral therapies will likely require a combination of drugs with complementary mechanisms of action to decrease the probability of selecting resistant viral mutants (Newcomer and Givens, 2013).

E2 mediates receptor recognition on the cell surface and is required for fusion of virus and cell membranes after the endocytic uptake of the virus during entry (Ronecker et al., 2008; Wang et al., 2004). Therefore, E2 is an attractive target for the development of antiviral strategies. Based on the recent determination of the crystal structure of BVDV E2 (El Omari et al., 2013; Li et al., 2013), we performed a computational virtual screening to select small-molecule ligands of E2. Molecules displaying antiviral activity against BVDV in cell culture were found to block virus entry by preventing internalization of the virus particle. This is the first report of a novel class of BVDV antivirals that act through inhibition of virus entry.

2-Methods

2.1 *Computational chemistry*

2.1.1 *Molecular system preparation*

All simulations were based on the crystal structure of the pestivirus ectodomain of the envelope glycoprotein from BVDV (PDB 2YQ2) (El Omari et al., 2013). Protein domains were designated from the N- to the C-terminus of E2 as I, II and III according to the nomenclature used by Li *et al.* (Li et al., 2013). The molecular system was described in terms of torsional coordinates using the ECEPP/3 force field (Nemethy et al., 1992) as implemented in the ICM program (version 3.7-2c, MolSoft LLC, La Jolla, CA) (Abagyan et al., 1994; Neves et al., 2012), and prepared in a similar fashion as in earlier works (Brand et al., 2013; He et al., 2012; Monti et al., 2009; Petrov et al., 2013). Succinctly, ligand charges were taken from the MMFF force field (Halgren, 1996). Hydrogen atoms were added to the receptor structure, followed by a local energy minimization in the dihedral space. All Asp and Glu residues were assigned a -1 charge, and all Arg and Lys residues were assigned a +1 charge. Histidine tautomers were assigned according to the hydrogen bonding pattern.

2.1.2 *Binding site identification*

ICM PocketFinder (An et al., 2005) and Megapocket 2.0 (An et al., 2005; Zhang et al., 2011) were used to detect druggable pockets. ICM PocketFinder explores possible binding pockets using an algorithm based on a transformation of the Lennard−Jones potential. The Megapocket 2.0 program uses interaction energies between the protein and a van der Waals probe to determine favorable binding sites. Both programs were used with default settings for all parameters.

2.1.3 *High-throughput docking*

Docking was performed within Site I after deleting all water molecules and co-factors using a flexible-ligand:rigid-receptor approach as implemented in ICM, where the receptor is represented by the

following six potential energy maps: electrostatic, hydrogen bond, hydrophobic, and three van der Waals. In the docking algorithm the ligand is considered flexible within the receptor field and subjected to global energy minimization so that both the intra- and inter-molecular energy of the ligand are minimized. After docking each molecule was assigned an empirical docking score according to its fit within the binding site (Totrov and Abagyan, 2001). To improve convergence of the global energy minimization step, high-throughput docking was performed twice, and using the ICM scoring function, the best score per molecule was kept.

Docked structures were refined in a ligand-steered fashion, were the ligand and side chains within 4.0 Å were sampled using an energy minimization protocol [for a detailed description cf. (Cavasotto and Abagyan, 2004; Cavasotto et al., 2008; Phatak et al., 2010)].

2.1.4 *Homology modeling*

The sequence of the E2 protein of cpBVDV genotype 2 was extracted from the sequence corresponding to the polyprotein with accession number AAA82981.1. The alignment with NADL strain of cpBVDV genotype 1 was performed using ICM, with an overall identity of 62%, and the structural model was built using ICM. The strain stemming from non-conserved residue substitution was relieved using a restraint local energy minimization (Domenech et al., 2013), in order to avoid unrealistic deformation of the system.

2.2 *Chemistry*

2.2.1 *General Information*

Compounds BI03 and PTC12 were obtained by chemical synthesis and purified by column chromatography carried out employing Merck silica gel (Kieselgel 60, 63-200 µm). Precoated silica gel plates F-254 were used for thin-layer analytical chromatography. Structural analysis by ^{1}H- and ^{13}C-NMR confirmed the identity of compounds and synthesis intermediates, and mass spectrometry was

used to determine their exact mass. NMR spectra were recorded on Bruker Biospin 600 MHz AVIII600, Bruker advance II 500MHZ and Bruker 300 MHZ spectrometers at room temperature. Chemical shifts (δ) are reported in ppm and coupling constants (J) in Hertz. The mass spectrometer utilized was a Xevo G2S QTOF (Waters Corporation, Manchester, UK) with an electrospray ionization (ESI) source. The mass spectrometer was operated in positive and negative ion modes with probe capillary voltages of 2.5 and 2.3 kV, respectively. The sampling cone voltage was 30 V. The source and desolvation gas temperatures were set to 120 and 350 °C, respectively. The nitrogen gas desolvation flow rate was 600 L h^{-1} and the cone desolvation flow rate was 10 L h^{-1}. The mass spectrometer was calibrated across the range of m/z 50−1200 using a 0.5 mM sodium formate solution prepared in 2- propanol/water (90:10 v/v). Data were drift corrected during acquisition using a leucine encephalin reference spray (LockSpray) infused at 2 μL min^{-1}. Data were acquired in the range of m/z 50−1200, and the scan time was set to 1 s. Data acquisition and processing were carried out using MassLynx, version 4.1 (Waters Corp., Milford, MA, USA). The purity (≥ 95%) of all final synthesized compounds was determined by reverse phase HPLC, using a Waters 2487 dual λ absorbance detector with a Waters 1525 binary pump and a Phenomenex Luna 5μ C18(2) 250 x 4.6 mm column. Samples were run at 1 mL/min using gradient mixtures of 5-100% of water with 0.1% trifluoroacetic acid (TFA) (A) and 10:1 acetonitrile:water with 0.1% TFA (B) for 22 min followed by 3 min at 100% B. UV spectra were measured with a Shimadzu 3600 UV/vis/NIR spectrophotometer.

2.2.2 *3-(1H-benzo[d]imidazol-2-yl)propan-1-ol (BI03)*

To a round-bottom flask containing the mixture of γ -butyrolactone (1) (0.2 ml, 2.16 mmol) and *o*-phenylene-diamine (2) (0.23 g, 2.16 mmol), were added concentrated HCl (2 mL) and water (3 mL). The mixture was stirred and heated to reflux for 24 h. The reaction mixture was neutralized with NaOH 1 M and extracted with ethyl acetate. The organic layer was sequentially washed with brine, dried over

anhydrous Na_2SO_4 and concentrated *in vacuo*. The crude product was purified by column chromatography (SiO_2, dichloromethane/methanol, 90:10) to give a white solid (0.20 g, 52 %). ^{1}H NMR (500 MHz, DMSO) δ 12.47 – 11.86 (m, 1H), 7.46 (dd, J = 5.1, 3.2 Hz, 2H), 7.15 – 7.06 (m, 2H), 4.86 – 4.44 (m, 1H), 3.50 (t, J = 6.3 Hz, 2H), 2.86 (t, J = 7.6 Hz, 2H), 1.96 – 1.87 (m, 2H). ^{13}C NMR (126 MHz, DMSO) δ 155.56, 121.49, 60.62, 31.23, 25.78. HR-MS (ES) calculated for $C_{10}H_{13}N_2O$ $[M+1]^+$ 177.1028, found 177.1158.

2.2.3- *3-(3,4-dimethoxybenzamido)-5-phenylthiophene-2-carboxamide (PTC12)*

(i) *3-amino-5-phenylthiophene-2-carboxamide (4)*

Methyl 3-amino-5-phenylthiophene-2-carboxylate (3) (0.25 g, 1.07 mmol), 2 M sodium hydroxide (1 mL) and methanol (3 mL) were heated at 70 °C for 24 h. The methanol was evaporated off and the residue was acidified with 2 M hydrochloric acid. Extraction into ethyl acetate (3 x 10 mL) followed by drying (Na_2SO_4) and evaporation of the solvent gave the acid and it is used directly for the following step (0.11 g, 49 %).

3-amino-5-phenylthiophene-2-carboxylic acid (0.11 g, 0.53 mmol) and thionyl chloride (4 mL) were heated at reflux for 1 h. After cooling, the excess thionyl chloride was evaporated off and final traces were removed by azeotroping with toluene. The residue was dissolved in acetonitrile (10 mL) and ammonia 28-30 % (2 mL) was added. After stirring for 1 h, the solvent was evaporated. The reaction mixture was extracted with ethyl acetate (3 x 15 mL). The organic layer was sequentially washed with brine (2 x 10 mL), dried over anhydrous Na_2SO_4 and concentrated *in vacuo*. The crude product was purified by column chromatography (SiO_2, dichloromethane/ethyl acetate 1:1) (0.0423 g, 37 %). ^{1}H NMR (600 MHz, CDCl3) δ 7.61 – 7.57 (m, 2H), 7.42 (t, J = 7.4 Hz, 2H), 7.38 (d, J = 7.2 Hz, 1H), 6.82 (s, 1H), 5.71 (s, 2H), 5.25 (s, 2H).

(ii) *3-(3,4-dimethoxybenzamido)-5-phenylthiophene-2-carboxamide (PTC12)*

A solution of 3,4-dimethoxybenzoyl chloride (0.04 g, 0.34 mmol) in THF (1 mL) was added dropwise to a mixture of 3-amino-5-phenylthiophene-2-carboxamide (0.04, 0.17 mmol) and DIPEA (0.06 ml, 0.34 mmol) in THF (2 mL) at 0 ^{o}C. The mixture was stirred at room temperature overnight. After this time, the THF was evaporated under reduced pressure and the crude product was purified by column chromatography (SiO2, dichloromethane/methanol 8:2) to yield a pale yellow solid (0.06 g, 20 %)

^{1}H NMR (500 MHz, $CDCl_3$) δ 11.99 (s, 1H), 8.63 (s, 1H), 7.72 (d, J = 7.1 Hz, 2H), 7.65 (s, 2H), 7.45 (d, J = 7.7 Hz, 2H), 7.41 (t, J = 7.2 Hz, 1H), 6.98 (d, J = 7.4 Hz, 1H), 5.63 (s, 2H), 4.00 (d, J = 16.4 Hz, 6H). ^{13}C NMR (126 MHz, CDCl3) δ 166.29, 164.04, 152.42, 149.11, 146.81, 145.55, 132.93, 129.24, 129.12, 126.28, 126.20, 120.60, 119.12, 118.88, 110.68, 110.58, 109.66, 56.01, 55.95.HR-MS (ES) calculated for $C_{20}H_{18}N_2O_4S$ $[M+1]^+$ 383.1066, found 383.1055.

Stock solutions of compounds were prepared in dimethyl sulfoxide (DMSO) at 50 mM and were then stored at -20 °C until use. Working dilutions of compounds were made in DMEM supplemented with 2% Horse Serum and antibiotics. In all cases DMSO concentration was kept to a maximum of 1%.

2.3 *Cells and viruses*

MDBK (*Bos taurus* kidney, ATCC CCL-22) and Vero (*Cercopithecus aethiops* kidney, ATCC CCL-81) cells were grown in Dulbecso's modified Eagle medium (DMEM) supplemented with 10% fetal bovine serum and antibiotics under 5% CO_2 at 37 °C. For infections, cells were cultivated in DMEM supplemented with 2% Horse serum and antibiotics under 5% CO_2 at 37 °C.

cpBVDV strain NADL was derived from the pACNR/NADL infectious cDNA clone (kindly provided by Dr. Charles Rice, The Rockefeller University) by electroporation of *in vitro* transcribed RNA into MDBK cells (Mendez et al., 1998). cpBVDV strain VS253 was amplified in MDBK cells.

Dengue Virus type 2 (DENV-2) was provided by Dr. Andrea Gamarnik (Fundación Instituto Leloir) and was amplified in Vero cells.

Bovine Herpes Virus type-1 (BHV-1) was provided by Dr. Ana Bratanich (Facultad de Ciencias Veterinarias, UBA) and was amplified in MDBK cells.

Virus titers were determined using end-point dilution assay in 96 well plates on MDBK or Vero cells, for BVDV and BHV-1 or DENV, respectively.

Viral stocks were stored at -70 ºC until use.

2.4 *Cytotoxicity and cytopathic effect reduction assays*

Cell viability assays were performed on confluent cell cultures in 96 well plates (approximately 15,000 cells per well). For each compound, cells were treated with serial dilutions of the compound and incubated at 37 °C for 3 days. Then, cell viability was measured using crystal violet staining. Briefly, cells were fixed with 10% formaldehyde, stained with crystal violet solution (20% Ethanol, 0.1% Crystal Violet), and after washing, the absorbance at 595 nm was recorded for each well in a spectrophotometer. Assays were conducted at least in triplicates, and the cytotoxic concentration 50 (CC_{50}) was estimated by a nonlinear regression fitting of the data as the compound concentration necessary to reduce cell viability by 50% compared to control non-treated cells.

Antiviral activity was evaluated by cytopathic effect reduction assays performed in confluent cultures in 96 well plates (approximately 15,000 cells per well). Cells were infected at a multiplicity of infection (moi) of 0.01 in the presence of serial dilutions of the compounds and incubated for 3 days at 37 °C. Then, cell viability was determined using crystal violet staining as a measure of the extension of cytopathic effect. Assays were conducted at least in triplicates and the inhibitory concentrations 50 (IC_{50}) for each compound were estimated by a nonlinear regression fitting of the data as the compound

concentration necessary to reduce cytopathic effect on MDBK cells by 50% compared to control infected and non-treated cells.

2.5 Construction of reporter cpBVDV/ N^{pro} GFP

Insertion of EGFP in between Npro and C genes of the infectios cDNA clone of cpBVDV NADL was designed as previously described by Fan et al. (Fan et al., 2008). First, a DNA fragment carrying the fusion of EGFP to FMDV2A followed by downstream SmaI and RsrII restriction sites was genetated by PCR and inserted into pGEM-T Easy (Promega) between EcoRI and PstI restriction sites. Next, a 672 bp fragment containing the 3' terminal portion of the BVDV IRES and the complete Npro sequence was amplified by PCR and inserted between unique SphI and EcoRI restriction sites of pGEM/EGFP-2A. A PCR product encompassing nucleotides 890 to 2838 of the NADL isolate of BVDV (accession no. AJ133738) was then cloned downstream of FMDV2A between unique SmaI and RsrII restriction sites to generate pGEM/Npro-EGFP-2A-C. The plasmid was digested with SphI and RsrII restriction enzymes to recover a 3363 DNA fragment that was cloned between unique SphI and RsrII restriction sites of pACNR/NADL to obtain reporter cpBVDV/N^{pro} GFP infectious cDNA clone. Stocks of cpBVDV/N^{pro} GFP were recovered from the supernatant of MDBK cells electroporated with *in vitro* transcribed RNA and titrated by flow cytometry.

2.6 Fluorescence microscopy

MDBK cells were seeded on glass coverslips and infected at an moi of 0.1. At the indicated times after infection, cells were thoroughly washed and fixed using paraformaldehyde (PFA) 4%. To analyze correlation between GFP and NS3 expression after infection with reporter cpBVDV/N^{pro} GFP, samples were first incubated with a mouse antibody against NS3, and were washed three times in PBS before addition of AlexaFluor conjugated secondary antibody. Cell nuclei were stained with DAPI and coverslips were then mounted onto glass slides using FluoroGuard Antifade Reagent (Bio-Rad).

Samples were visualized under a Nikon Eclipse 80i fluorescence microscope equipped with a DS-Qi1Mc camera.

2.7 Flow cytometry

MDBK cells were seeded onto 24 well plates, infected with cpBVDV/N^{pro} GFP and treated as indicated. For flow cytometry analysis, cells were thoroughly washed, lifted with trypsin 0.05% and fixed using PFA 4%. The fluorescence signal was measured using a flow cytometer (CyFlow® Space, Partec) at a detection spectrum of 488 nm. Data were analyzed in the FlowJo 7.6.2 software package.

2.8 Study of the mechanism of action of antiviral compounds

Time of drug addition and entry assays were performed to study the mechanism of action using compound PTC12 at 1 µM and compound BI03 at 50 µM.

2.8.1 Time of drug addition

Time of addition assays were performed on MDBK cells seeded onto 24 well plates infected with cpBVDV/N^{pro} GFP at an moi of 0.5. The effect of compound depending on the time of addition was tested in three stages: prior to viral infection (Pre addition), during viral infection (Co addition) and after viral infection (Post addition). In the Pre addition stage, cells were incubated with compound for 2 hours under 5% CO_2 at 37 °C. Then the cells were thoroughly washed, infected with cpBVDV/N^{pro} GFP and incubated for 2 hours at 37 °C. In the Co addition stage, compound and cpBVDV/N^{pro} GFP were added simultaneously to the cells and infection was allowed to proceed for 2 hours at 37 °C under 5% CO_2 at 37 °C. Then cells were thoroughly washed and incubated with compound for 24 hours under 5% CO_2 at 37 °C. In the Post addition stage cells were infected with cpBVDV/N^{pro} GFP and incubated for 2 hours under 5% CO_2 at 37 °C. Then cells were thoroughly washed and compound was added immediately (2 hours post infection), or at 4 or 6 hours post infection. Then infection was allowed to proceed in the presence of compound for 24 hours under 5% CO_2 at 37 °C. All samples were processed

for flow cytometry analysis at 24 hours post infection. The percentages of GFP positive cells in treated samples were compared to control non-treated samples to calculate the relative percentage of GFP positive cells.

2.8.2 Entry assays

(i) Quantification of foci of infection to evaluate the effect of compounds on the attachment and internalization steps

The effect of compounds on the attachment and internalization steps during entry was initially assessed quantifying the number of infection foci after infection with cpBVDV/N^{pro} GFP (moi 0.5). To test the effect of compounds on the attachment step, MDBK cells were plated on glass coverslips and infected in either infection medium containing compound or medium without compound on ice to allow for virus attachment. After 1 h attachment, medium containing non-attached virus and compound was removed and cell cultures were thoroughly washed with PBS. Then, fresh medium was added and the cells were incubated for 48 hours under 5% CO_2 at 37 °C.

To test the effect of compounds on the internalization step, MDBK cells were infected and after 1 h attachment on ice, medium containing non-attached virus was removed, cell cultures were thoroughly washed with PBS and medium containing compound or medium without compound was added. Infected cells were incubated for 1 hour under 5% CO_2 at 37 °C to allow for virus internalization and then thoroughly washed with PBS before fresh medium was added and cells were incubated for 48 hours under 5% CO_2 at 37 °C.

After 48 hours of incubation cells were fixed and processed for fluorescence microscopy. Viral foci for each treatment were quantified on five fields acquired using a 4x objective by using the analytical tools of the ImageJ software. Appropriate threshold of green channel identified objects corresponding to GFP expression on cpBVDV/N^{pro} GFP infected cells. We next used the dilate tool and

the particle analyzer to filter objects according to size and shape and create a mask displaying only foci that cover more than 5 infected cells. Finally we counted the number of foci obtained according to the filter. We conducted three independent experiments and at least 30-50 foci were quantified in the control in each case. The number of foci in treated samples was compared to control non-treated samples to calculate the relative percentage of foci of infection.

(ii) Quantification of attached virus

To specifically test the effect of compounds on the attachment step, MDBK cells were seeded onto 12 well plates and infected with cpBVDV/N^{pro} GFP (moi 0.25) in either medium containing compound or medium without compound for 1 hour on ice to allow for virus attachment. After 1 h attachment, medium containing non-attached virus and compound (treated cultures) was removed and cell cultures were thoroughly washed with PBS. Then cells were lifted by scraping and subjected to three freeze and thaw cycles. Cell lysates were clarified by low speed centrifugation and used to infect a fresh monolayer of MDBK cells. Infection was allowed to proceed for 48 hours under 5% CO_2 at 37 °C and samples were then processed for flow cytometry analysis.

(iii) Quantification of internalized virus

To test the effect of compounds on the internalization step, MDBK cells were infected with cpBVDV/N^{pro} GFP (moi 0.25) in medium without compound and incubated for 1 hour on ice. Medium containing non-attached virus was then removed and cell cultures were thoroughly washed with PBS. Medium containing compound was added to treated cells and medium without compound was added to control cells. Samples were incubated for 1 hour under 5% CO_2 at 37 °C to allow virus internalization, and then were thoroughly washed with PBS and treated with 0.25% Trypsin-EDTA for 15 minutes under 5% CO_2 at 37 °C. Then the cell suspension was collected into a tube, trypsin was inactivated with 4 mM PMSF/6% horse serum in PBS, and the cells were washed with PBS. This suspension was used to

inoculate a fresh monolayer of MDBK cells that were incubated for 48 hours under 5% CO_2 at 37 °C and then processed for flow cytometry analysis.

2.9 Statistical analysis

Curve fitting and statistical analysis were performed with GraphPad Prism 5 software. Sets of data were compared using unpaired t-test or one way ANOVA with Dunnett post test as indicated for each case.

3-Results

3.1-Computer-aided discovery of novel inhibitors

Structure-based virtual screening (SBVS) has been widely used in drug discovery (Cavasotto and Orry, 2007; Jorgensen, 2009, 2012; Shoichet et al., 2002; Spyrakis and Cavasotto, 2015). The available structural data of the BVDV virus envelope protein E2 opened up the possibility to identify antiviral agents interfering with early steps of BVDV virus infection. Our multistep hierarchical SBVS strategy includes the identification of new binding sites and docking-based virtual screening searches. Programs ICM PocketFinder (An et al., 2005) and Megapocket 2.0 (An et al., 2005; Zhang et al., 2011) were used to detect druggable pockets in the envelope protein E2. Two major possible binding sites were found: site I located between domains I and II, and site II located at the dimer interface in domain IIIc. In principle, site I was selected because it has the largest predicted pocket volumes (~700 $Å^3$) and resulted more appropriate for ligand binding (Figure 1).

Docking-based virtual screening was performed using approximately 110,000 small-molecules from the Maybridge database to identify ligands of E2 (PDB code: 2YQ2, chain A) using the ICM software, which proved successful for finding hits on several other targets (Cavasotto et al., 2008; Cavasotto et al., 2006; Chan et al., 2013; Leal et al., 2017; Sun et al., 2014). An initial ADME filter (Jorgensen, 2005) was imposed, in order to retain only potentially non-toxic and druggable molecules. The selected molecules were subjected to independent parallel high-throughput docking (HTD) cycles and the best ICM docking score per molecule was kept (Cavasotto and Abagyan, 2004; Kovacs et al., 2005). The top 100 ranked compounds were subjected to manual inspection using the following criteria: (i) scaffold diversity, (ii) commercial availability, and (iii) synthetic tractability for potential modifications. All molecules containing unwanted structural features were removed such as those with readily hydrolyzable and/or highly electrophilic functional groups. Finally, 10 compounds were taken

into consideration for *in vitro* study and were either purchased or synthesized. In particular, compounds **BI03** and **PTC12** were prepared and the synthetic routes are shown in Scheme 1. Compound **BI03** was prepared by reacting of ɣ-butyrolactone (**1**) and *o*-phenylenediamine (**2**) in acid conditions in a good yield (Indusegaram et al., 2003) (Scheme 1A). For the synthesis of **PTC12** (Scheme 1B), we started from commercially available methyl 3-amino-5-phenylthiophene-2-carboxylate (**3**), which was hydrolyzed under basic conditions to afford the corresponding thiophene carboxylic acid. The intermediate was converted to the aminoamides *via* thionyl chloride treatment followed by reaction with ammonia (**4**). The aminoamide was reacted with of 3,4-dimethoxybenzoyl chloride to give the desired compound in a good yield.

3.2- In vitro screening of antiviral activity

First, we tested the molecules selected in the virtual screening for cytotoxicity. To this end we treated MDBK cells with serial dilutions of the compounds and measured cell viability using crystal violet staining. Only one compound displayed cytotoxic concentration 50 (CC_{50}) below 25 µM and was excluded from further analysis.

In order to screen molecules for antiviral activity we used a cytopathic effect reduction assay in 96 well format. MDBK cells were infected with the NADL strain of cpBVDV genotype 1a in the presence of compounds, and the inhibition of the cytopathic effect induced by BVDV infection was measured three days after infection by comparing the extension of cytopathic effect of control cells and cells treated with increasing amounts of compound using crystal violet staining. The inhibitory concentrations 50 (IC_{50}s) for the compounds tested in the assay were estimated from curves constructed by plotting the percentage of inhibition versus the concentration of compound. Phenyl thiophene carboxamide derivative compound PTC12 was the most active antiviral displaying an IC50 of 0.30 ±

0.13 μM against the virus (Figure 2A and B) and CC_{50} of 89.52 ± 1.15 μM (selectivity index (SI) = 294) (Table 1).

To extend our analysis, we tested compound PTC12 against the VS253 strain of cpBVDV genotype 2. Compared to the reference NADL strain used in the screening, the VS253 strain appeared more sensitive to the antiviral effect of the compound (Table 1), indicating that compound PTC12 is capable of inhibiting both genotypes of the virus.

Next we asked whether antiviral activity of the compound was specific to BVDV and tested compound PTC12 against dengue virus (DENV, another member of the *Flaviviridae* family) and against bovine herpes virus 1 (BHV-1, another bovine virus that replicates in MDBK cells). Activity of the compound against DENV was tested in Vero cells in the range of concentrations that proved to be active against BVDV. Cytopathic effect reduction assay showed that the compound displayed modest inhibition of DENV in this range of concentrations (Figure 3A) that was also found to be not toxic to Vero cells (data not shown). In turn, compound PTC12 did not display antiviral activity against BHV-1 in MDBK cells (Figure 3A). Altogether, these set of data suggest that antiviral activity of compound PTC12 is in part specific to BVDV and that the compound does not induce a general antiviral state in MDBK cells.

3.3-Design and construction of a reporter BVDV

We generated a reporter BVDV expressing GFP to aid the study of the mechanism of action of antiviral compounds. The sequence encoding EGFP followed by the foot and mouth disease virus autoprotease 2A (FMDV2A) was inserted into the infectious cDNA clone of cytopathic BVDV NADL between the terminal protease N^{pro} and the capsid protein C (cpBVDV/N^{pro}-GFP, Figure 4A and B), so that GFP is released from the viral polyprotein into the cytoplasm of infected cells. Genome-length recombinant RNA was transcribed *in vitro* from the infectious clone and used to transfect MDBK cells.

GFP expression of transfected cells was checked by fluorescence microscopy, and the supernatant was collected and used to infect a new monolayer of cells. Immunofluorescence staining of infected cells with anti NS3 antibody showed that GFP expressing cells were also stained for BVDV NS3, indicating that GFP expression coincided with BVDV replication (Figure 4C). Time course of infection showed that at 24 hours expression of GFP was limited to individual cells, thus reflecting virus replication in the primary infected cell (Figure 4D, left panel). As a result of spread of infection to neighboring cells, GFP expressing cells formed foci comprising 10-12 nuclei at 48 hours (Figure 4D, middle panel). By 72 hours, cytopathic effect was evident (Figure 4D, right panel). We then used the 48 hours time point to number foci of infection and quantify virus infectious units. Fluorescence microscopy images were acquired with a 4x objective and the number of foci was counted using computer assisted image analysis (Figure 4E and Materials and Methods). As an alternative means of quantification, expression of GFP was followed as a function of time by flow cytometry (Figure 4F). GFP-expressing MDBK cells could be detected at 24 hours post infection and the percentage of GFP positive cells increased at 48 hours, reflecting virus replication and the spread of infection. At 72 hours, as the cytopathic effect became visible the percentage of GFP positive cells did not increase. Therefore, the expression of GFP from the recombinant BVDV genome served as a quantitative reporter of virus replication that could be used both in fluorescence microscopy and cell cytometry analyses.

3.4-Time of drug addition experiments

Next, we tested compound PTC12 against the reporter BVDV. To this end, we performed infections of MDBK cells with cpBVDV/N^{pro}-GFP in the presence of increasing amounts of compound PTC12 and quantified the percentage of infected cells by flow cytometry at 48 hours post infection. Compared to untreated cells, we observed a dose-dependent decrease in the percentage of GFP positive cells showing inhibition of BVDV infection (Figure 5A). Furthermore, the 50% of inhibition was

achieved at a compound concentration similar to the IC_{50} calculated in the cytopathic effect reduction assay. Therefore, reporter BVDV was used to study the mechanism of action of antiviral compounds.

To gain insight into the mechanism of action of compound PTC12, we first performed time of drug addition experiments (Figure 5B). Cells were infected with cpBVDV/N^{pro}-GFP and after washing infection at 2 hours the percentage of GFP-expressing cells was measured 24 hours post infection to assess replication in a single cycle (see Figure 4D). When cells were pretreated with PTC12 for 2 hours before infection and then washed (pre addition), no differences in the percentage of GFP expressing cells were observed compared to the untreated control. In turn, infection in the presence of PTC12 (co-addition) resulted in a 2.5-fold reduction of GFP expressing cells. In contrast, only a slight reduction of GFP expressing cells was observed when the compound was added at 2 hours after infection, and no reduction was observed at 4 or 6 hours (post-addition). These results suggest that compound PTC12 acts against BVDV at an early stage of infection.

3.5-Attachment and internalization assays

Based on the selection of E2 as the target for drug design and the results of the time of drug addition assay showing that only co treatment of BVDV with compound PTC12 inhibited infection (see Figure 5B), we speculated that the compound could act either as a virucidal agent or through blocking of virus entry. Treatment of BVDV with PTC12 prior to infection did not affect virus infectivity, indicating that the compound was not acting as a virucidal agent (data not shown). Therefore, we focused on the study of the effect of the compound on virus entry. Entry of BVDV involves initial attachment of the virus to the host cell mediated by the interaction of virus with glycosaminoglycans (Iqbal et al., 2000; Iqbal and McCauley, 2002) and specific receptors (Krey et al., 2006; Maurer et al., 2004), and internalization through clathrin-mediated endocytosis (Krey et al., 2005; Lecot et al., 2005). Fusion of virus and host membranes results in the release of the RNA genome into the cytoplasm of the cell. To

test the effect of compound PTC12 on virus entry, we first used an approach based on the quantification of foci of infection by fluorescence microscopy after virus infection and antiviral treatment at the stages of attachment and internalization. Cells were incubated with reporter BVDV for 1 hour on ice to allow virus attachment, and after extensive washing to remove non attached virus, foci of infection were quantified at 48 hours of infection (see Figure 4E). To target virus attachment, the compound was incubated with the virus during the first hour on ice. Both non-attached virus and compound were washed after the attachment step and the infection proceeded for additional 48 hours. On the other hand, to target virus internalization, the compound was added after removal of non-attached virus for one hour at 37 ºC and then washed to allow infection to proceed in the absence of compound. Compared to the untreated control, addition of compound during attachment did not significantly reduce the number of foci of infection. In contrast, addition of the compound during internalization resulted in a ~3-fold reduction in the number of foci, suggesting that compound PTC12 targets a post-attachment step (Figure 6A).

To confirm our results, we used complementary assays to evaluate the activity of the compound at the stages of attachment and internalization. In the attachment assay, reporter virus was allowed to attach to MDBK cells for one hour on ice and, after washing of non attached virus, cells were collected and lysed. The clarified supernatant was then used to infect a new monolayer of cells, and the percentage of GFP positive cells quantified at 48 hours by flow cytometry. Similar to our previous observation, we found that the percentage of GFP positive cells was comparable between treated cells and untreated control cells (Figure 6B). In the internalization assay, MDBK cells were infected with reporter BVDV for 1 hour on ice, and after washing of non attached virus, shifted to 37 ºC for an additional hour to allow internalization. Cells were then treated with trypsin to remove non-internalized virus, collected in cell culture media, and plated onto a new monolayer of MDBK cells. Quantification

of the percentage of GFP positive cells by flow cytometry at 48 hours showed that treatment with compound PTC12 during internalization resulted in a ~10-fold reduction in the percentage of infected cells compared to the untreated control (Figure 6C). In line with our previous result, this observation confirmed that compound PTC12 specifically targets internalization of the virus.

3.6-Active compounds emerging from the virtual screen share a common mechanism of action

We next reasoned that active compounds identified in the virtual screen to target the site located between domains I and II of E2 should have the same mechanism of action that compound PTC12. To test this hypothesis we analyzed the mechanism of action of benzimidazole derivative compound **BI03**. The IC_{50} for compound BI03 calculated in the cytopathic effect reduction assay was 17.6 ± 6.43 μM (Figure 7A and Table 1). The time of addition assay confirmed that compound BI03 acted at an early stage of infection (Figure 7B). Furthermore, evaluation of the effect of compound BI03 at the stages of attachment and internalization showed that, similar to compound PTC12, this compound specifically inhibited internalization of BVDV (Figure 7C, D and E). Altogether, our results uncover a new class of BVDV antivirals that inhibit virus entry by targeting internalization of the virus into the host cell.

3.7-Docking analysis of E2-compounds complex.

To characterize the likely interaction between compounds **BI03** and **PTC12** within their binding site, their docking pose is shown in (Figure 8A). These two compounds may bind in the pocket between domains I and II, in an area surrounded by mainly polar amino acid residues including R154, P105, D91, Q87, Q89, V153, R61, and T60. Both compounds display a Π-cation stacking interaction with R154 (Figure 8B and C and Supplementary Figure 1). For the most active hit **PTC12,** 5-phenylthiophene-2-carboxamide is well buried within the pocket, and the amide group of the ligand forms hydrogen bonds with Q89 and Q87.

Since PTC12 exhibits activity against genotype 2 of the virus, a structural model of BVDV genotypoe 2 envelope protein E2 was built by homology, and its complex with PTC12 refined (Figure 8D and Supplementary Figure 1). The binding site is overall conserved, the differences limited to an exposed Q87 mutated into T85, and T60 into P58, where the latter mutation enhances the hydrophobic interaction between E2 and the ligand; it is also observed the conserved substitution R61→K59. Thus, the structure of E2 binding site from BVDV genotype 2 supports the *in vitro* data showing that PTC12 is also active against genotype 2 of the virus (see Table 1).

Discussion

Virus glycoproteins on the surface of the virion mediate attachment to cellular receptor(s) and fusion of viral and cellular membranes to direct virus entry to the host cell. Targeting of envelope proteins function is a common strategy for antiviral therapy. For instance, computer-aided drug design has been successfully employed to identify small-molecule ligands of the envelope glycoprotein E of DENV. DENV protein E mediates both attachment to receptor and fusion, and binding of small molecules to a hydrophobic pocket that is occupied by a detergent in the crystal structure of the protein blocks the fusion step during entry (Kampmann et al., 2009; Poh et al., 2009; Wang et al., 2009). In the case of pestiviruses, envelope proteins E1 and E2 are responsible for virus entry. E2 is known to mediate receptor attachment whereas a heterodimer of E1 and E2 is required for fusion (Ronecker et al., 2008; Wang et al., 2004). However, the details of the workings of the fusion machinery of BVDV are still ill defined. The recent determination of the crystal structure of E2 (El Omari et al., 2013; Li et al., 2013) has opened the possibility for the design of antiviral strategies that target the function of E2. Following a computer-aided drug design strategy, we identified a druggable site in the interface of domains I and II of E2 and selected small molecule ligands of the protein. As a result of virtual screening and *in vitro* assay of antiviral activity of top ranked molecules, we identified two compounds with anti BVDV activity in the micromolar range. Docking of antiviral compounds to the binding site in E2 revealed the presence of common interactions between compounds **BI03** and **PTC12**, and the viral protein. Furthermore, these compounds shared a common mechanism of action, blocking internalization of BVDV. Structural studies have shown that the domain I–II interface appears flexible and that domain I of E2 becomes disordered at low pH, suggesting that similar to flavivirus and alphavirus fusion proteins, E2 may undergo a conformational change that exposes a still unidentified fusion motif that inserts into the endosomal membrane (El Omari et al., 2013). Thus, we speculate that binding of antiviral

compounds into the pocket formed in the domain I-II interface may lock the conformation of the protein blocking fusion. Nevertheless, the molecular target of active compounds still needs to be confirmed. *In vitro* binding assays with recombinant E2 and selection of resistant viruses will be the object of future investigation to validate the target of compounds.

Several recombinant pestivirus genomes have been previously designed that express reporter genes (Arenhart et al., 2014; Fan and Bird, 2012; Fan et al., 2008; Li et al., 2016; Shen et al., 2014). In fact, stable expression of heterologous genes was achieved using non-cytopathic strains of BVDV carrying GFP or luciferase coding sequences inserted between N^{pro} and C (Arenhart et al., 2014; Fan et al., 2008). Here, we followed the same strategy to construct a recombinant virus expressing GFP in the context of the full-length genome of the cytopathic biotype of the NADL strain of BVDV. We showed that the virus was a useful tool to study the mechanism of action of antiviral compounds using fluorescence microscopy or flow cytometry to quantitate GFP expression as a reporter of BVDV replication.

Antiviral treatment with cationic aromatic compound DB772 was shown to prevent acute infection of BVDV and to decrease viral titers in PI calves. However, resistant isolates rapidly arose after administration of the compound. Analysis of mutations in DB722 resistant isolates suggests that the compound acts through inhibition of the RNA dependent RNA polymerase of the virus (Newcomer et al., 2012; Newcomer et al., 2013b). Here we describe a new class of BVDV antivirals with a separate mechanism of action. Compound PTC12 inhibited virus entry and proved to be active against genotypes 1 and 2 of the virus. Therefore, it is feasible to design combination antiviral therapies that use polymerase inhibitors together with entry inhibitors to limit the selection of mutations associated to antiviral resistance.

In conclusion, we took a computer-aided approach to identify compound PTC12 as a potent inhibitor of BVDV replication. Using the backbone of the cytopathic biotype of the NADL strain of BVDV we designed a reporter virus expressing GFP. Detection of GFP was sensitive enough to monitor a single cycle of virus replication allowing for detailed studies of the mechanism of action of antiviral compounds. In agreement with selection of the envelope protein E2 as the target for computer design, we found that compound PTC12 blocked virus entry at the stage of internalization. Thus, compound PTC12 can also serve to define the molecular details of the function of E2 beyond receptor recognition.

Acknowledgments

This work was supported by the National Agency for the Promotion of Science and Technology (ANPCyT) grants to DEA (PICT2014-2213) and MB (PICT2014-1884) and the National Scientific and Technical Research Council (CONICET) grant to MB, CNC and DEA (PIP2014 11220130100721), and FOCEM-Mercosur (COF 03/11).

DEA is grateful to Juan Ugalde for his continued support. MB thanks William Jorgensen for providing an academic license for QikProp software. CNC thanks Molsoft LLC for providing an academic license for the ICM program. The authors thank the National System of High Performance Computing (Sistemas Nacionales de Computación de Alto Rendimiento, SNCAD), the Computational Centre of High Performance Computing (Centro de Computación de Alto Rendimiento, CeCAR) for granting use of their computational resources and Dr. Mariela Videla for technical assistance and use of mass spectrometry facility at CIBION.

References

Abagyan, R., Totrov, M., Kuznetsov, D., 1994. ICM—A new method for protein modeling and design: Applications to docking and structure prediction from the distorted native conformation. Journal of Computational Chemistry 15, 488-506.
An, J., Totrov, M., Abagyan, R., 2005. Pocketome via comprehensive identification and classification of ligand binding envelopes. Molecular & cellular proteomics : MCP 4, 752-761.
Arenhart, S., Flores, E.F., Weiblen, R., Gil, L.H., 2014. Insertion and stable expression of Gaussia luciferase gene by the genome of bovine viral diarrhea virus. Research in veterinary science 97, 439-448.
Becher, P., Tautz, N., 2011. RNA recombination in pestiviruses: cellular RNA sequences in viral genomes highlight the role of host factors for viral persistence and lethal disease. RNA biology 8, 216-224.
Brand, C.S., Hocker, H.J., Gorfe, A.A., Cavasotto, C.N., Dessauer, C.W., 2013. Isoform selectivity of adenylyl cyclase inhibitors: characterization of known and novel compounds. The Journal of pharmacology and experimental therapeutics 347, 265-275.
Callens, N., Brugger, B., Bonnafous, P., Drobecq, H., Gerl, M.J., Krey, T., Roman-Sosa, G., Rumenapf, T., Lambert, O., Dubuisson, J., Rouille, Y., 2016. Morphology and Molecular Composition of Purified Bovine Viral Diarrhea Virus Envelope. PLoS pathogens 12, e1005476.
Cavasotto, C.N., Abagyan, R.A., 2004. Protein flexibility in ligand docking and virtual screening to protein kinases. Journal of molecular biology 337, 209-225.
Cavasotto, C.N., Orry, A.J., 2007. Ligand docking and structure-based virtual screening in drug discovery. Current topics in medicinal chemistry 7, 1006-1014.
Cavasotto, C.N., Orry, A.J., Murgolo, N.J., Czarniecki, M.F., Kocsi, S.A., Hawes, B.E., O'Neill, K.A., Hine, H., Burton, M.S., Voigt, J.H., Abagyan, R.A., Bayne, M.L., Monsma, F.J., Jr., 2008. Discovery of novel chemotypes to a G-protein-coupled receptor through ligand-steered homology modeling and structure-based virtual screening. Journal of medicinal chemistry 51, 581-588.
Cavasotto, C.N., Ortiz, M.A., Abagyan, R.A., Piedrafita, F.J., 2006. In silico identification of novel EGFR inhibitors with antiproliferative activity against cancer cells. Bioorganic & medicinal chemistry letters 16, 1969-1974.
Chan, F.Y., Sun, N., Neves, M.A., Lam, P.C., Chung, W.H., Wong, L.K., Chow, H.Y., Ma, D.L., Chan, P.H., Leung, Y.C., Chan, T.H., Abagyan, R., Wong, K.Y., 2013. Identification of a new class of FtsZ inhibitors by structure-based design and in vitro screening. Journal of chemical information and modeling 53, 2131-2140.
Collett, M.S., Larson, R., Belzer, S.K., Retzel, E., 1988. Proteins encoded by bovine viral diarrhea virus: the genomic organization of a pestivirus. Virology 165, 200-208.
Domenech, R., Hernandez-Cifre, J.G., Bacarizo, J., Diez-Pena, A.I., Martinez-Rodriguez, S., Cavasotto, C.N., de la Torre, J.G., Camara-Artigas, A., Velazquez-Campoy, A., Neira, J.L., 2013. The histidine-phosphocarrier protein of the phosphoenolpyruvate: sugar phosphotransferase system of Bacillus sphaericus self-associates. PloS one 8, e69307.
El Omari, K., Iourin, O., Harlos, K., Grimes, J.M., Stuart, D.I., 2013. Structure of a pestivirus envelope glycoprotein E2 clarifies its role in cell entry. Cell reports 3, 30-35.
Fan, Z.C., Bird, R.C., 2012. Development of a reporter bovine viral diarrhea virus and initial evaluation of its application for high throughput antiviral drug screening. Journal of virological methods 180, 54-61.

Fan, Z.C., Dennis, J.C., Bird, R.C., 2008. Bovine viral diarrhea virus is a suitable viral vector for stable expression of heterologous gene when inserted in between N(pro) and C genes. Virus research 138, 97-104.
Fulton, R.W., Ridpath, J.F., Confer, A.W., Saliki, J.T., Burge, L.J., Payton, M.E., 2003. Bovine viral diarrhoea virus antigenic diversity: impact on disease and vaccination programmes. Biologicals : journal of the International Association of Biological Standardization 31, 89-95.
Halgren, T.A., 1996. Merck molecular force field. I-V. Journal of Computational Chemistry 17, 490-641.
He, W., Elizondo-Riojas, M.A., Li, X., Lokesh, G.L., Somasunderam, A., Thiviyanathan, V., Volk, D.E., Durland, R.H., Englehardt, J., Cavasotto, C.N., Gorenstein, D.G., 2012. X-aptamers: a bead-based selection method for random incorporation of druglike moieties onto next-generation aptamers for enhanced binding. Biochemistry 51, 8321-8323.
Indusegaram, S., Katsifis, A.G., Ridley, D.D., Vonwiller, S.C., 2003. Nitrogen versus Oxygen Group Protection in Hydroxypropylbenzimidazoles. Australian Journal of Chemistry 56, 819-827.
Iqbal, M., Flick-Smith, H., McCauley, J.W., 2000. Interactions of bovine viral diarrhoea virus glycoprotein E(rns) with cell surface glycosaminoglycans. The Journal of general virology 81, 451-459.
Iqbal, M., McCauley, J.W., 2002. Identification of the glycosaminoglycan-binding site on the glycoprotein E(rns) of bovine viral diarrhoea virus by site-directed mutagenesis. The Journal of general virology 83, 2153-2159.
Jorgensen, W.L., 2005. QikProp, v 3.0; Schrödinger LLC, New York.
Jorgensen, W.L., 2009. Efficient drug lead discovery and optimization. Accounts of chemical research 42, 724-733.
Jorgensen, W.L., 2012. Challenges for academic drug discovery. Angewandte Chemie 51, 11680-11684.
Kampmann, T., Yennamalli, R., Campbell, P., Stoermer, M.J., Fairlie, D.P., Kobe, B., Young, P.R., 2009. In silico screening of small molecule libraries using the dengue virus envelope E protein has identified compounds with antiviral activity against multiple flaviviruses. Antiviral research 84, 234-241.
Kovacs, J.A., Cavasotto, C.N., Abagyan, R.A., 2005. Conformational Sampling of Protein Flexibility in Generalized Coordinates: Application to ligand docking. J. Comp. Theor. Nanosci. 2, 354-361.
Krey, T., Himmelreich, A., Heimann, M., Menge, C., Thiel, H.J., Maurer, K., Rumenapf, T., 2006. Function of bovine CD46 as a cellular receptor for bovine viral diarrhea virus is determined by complement control protein 1. J Virol 80, 3912-3922.
Krey, T., Thiel, H.J., Rumenapf, T., 2005. Acid-resistant bovine pestivirus requires activation for pH-triggered fusion during entry. J Virol 79, 4191-4200.
Lanyon, S.R., Hill, F.I., Reichel, M.P., Brownlie, J., 2014. Bovine viral diarrhoea: pathogenesis and diagnosis. Veterinary journal 199, 201-209.
Leal, E.S., Aucar, M.G., Gebhard, L.G., Iglesias, N.G., Pascual, M.J., Casal, J.J., Gamarnik, A.V., Cavasotto, C.N., Bollini, M., 2017. Discovery of novel dengue virus entry inhibitors via a structure-based approach. Bioorganic & medicinal chemistry letters 27, 3851-3855.
Lecot, S., Belouzard, S., Dubuisson, J., Rouille, Y., 2005. Bovine viral diarrhea virus entry is dependent on clathrin-mediated endocytosis. J Virol 79, 10826-10829.
Li, Y., Wang, J., Kanai, R., Modis, Y., 2013. Crystal structure of glycoprotein E2 from bovine viral diarrhea virus. Proceedings of the National Academy of Sciences of the United States of America 110, 6805-6810.

Li, Y., Wang, X., Sun, Y., Li, L.F., Zhang, L., Li, S., Luo, Y., Qiu, H.J., 2016. Generation and evaluation of a chimeric classical swine fever virus expressing a visible marker gene. Archives of virology 161, 563-571.
Lindenbach, B.D., Thiel, H.-J., Rice, C.M., 2007. Flaviviridae: The viruses and their replication, 5th ed. Lippincott-Raven, Philadelphia.
Maurer, K., Krey, T., Moennig, V., Thiel, H.J., Rumenapf, T., 2004. CD46 is a cellular receptor for bovine viral diarrhea virus. J Virol 78, 1792-1799.
Mendez, E., Ruggli, N., Collett, M.S., Rice, C.M., 1998. Infectious bovine viral diarrhea virus (strain NADL) RNA from stable cDNA clones: a cellular insert determines NS3 production and viral cytopathogenicity. J Virol 72, 4737-4745.
Monti, M.C., Casapullo, A., Cavasotto, C.N., Tosco, A., Dal Piaz, F., Ziemys, A., Margarucci, L., Riccio, R., 2009. The binding mode of petrosaspongiolide M to the human group IIA phospholipase A(2): exploring the role of covalent and noncovalent interactions in the inhibition process. Chemistry 15, 1155-1163.
Nemethy, G., Gibson, K.D., Palmer, K.A., Yoon, C.N., Paterlini, G., Zagari, A., Rumsey, S., Scheraga, H.A., 1992. Energy parameters in polypeptides. 10. Improved geometrical parameters and nonbonded interactions for use in the ECEPP/3 algorithm, with application to proline-containing peptides. The Journal of Physical Chemistry 96, 6472-6484.
Neves, M.A.C., Totrov, M., Abagyan, R., 2012. Docking and scoring with ICM: the benchmarking results and strategies for improvement. Journal of Computer-Aided Molecular Design 26, 675-686.
Newcomer, B.W., Chamorro, M.F., Walz, P.H., 2017. Vaccination of cattle against bovine viral diarrhea virus. Veterinary microbiology 206, 78-83.
Newcomer, B.W., Givens, M.D., 2013. Approved and experimental countermeasures against pestiviral diseases: Bovine viral diarrhea, classical swine fever and border disease. Antiviral research 100, 133-150.
Newcomer, B.W., Marley, M.S., Galik, P.K., Walz, P.H., Zhang, Y., Riddell, K.P., Dykstra, C.C., Boykin, D.W., Kumar, A., Cruz-Espindola, C., Boothe, D.M., Joiner, K.S., Givens, M.D., 2012. Antiviral treatment of calves persistently infected with bovine viral diarrhoea virus. Antiviral chemistry & chemotherapy 22, 171-179.
Newcomer, B.W., Marley, M.S., Galik, P.K., Zhang, Y., Riddell, K.P., Boykin, D.W., Kumar, A., Kuhnt, L.A., Gard, J.A., Givens, M.D., 2013a. Effect of treatment with a cationic antiviral compound on acute infection with bovine viral diarrhea virus. Canadian journal of veterinary research = Revue canadienne de recherche veterinaire 77, 170-176.
Newcomer, B.W., Neill, J.D., Marley, M.S., Ridpath, J.F., Givens, M.D., 2013b. Mutations induced in the NS5B gene of bovine viral diarrhea virus by antiviral treatment convey resistance to the compound. Virus research 174, 95-100.
Petrov, R.R., Knight, L., Chen, S.R., Wager-Miller, J., McDaniel, S.W., Diaz, F., Barth, F., Pan, H.L., Mackie, K., Cavasotto, C.N., Diaz, P., 2013. Mastering tricyclic ring systems for desirable functional cannabinoid activity. European journal of medicinal chemistry 69, 881-907.
Phatak, S.S., Gatica, E.A., Cavasotto, C.N., 2010. Ligand-steered modeling and docking: A benchmarking study in class A G-protein-coupled receptors. Journal of chemical information and modeling 50, 2119-2128.
Poh, M.K., Yip, A., Zhang, S., Priestle, J.P., Ma, N.L., Smit, J.M., Wilschut, J., Shi, P.Y., Wenk, M.R., Schul, W., 2009. A small molecule fusion inhibitor of dengue virus. Antiviral research 84, 260-266.
Ridpath, J.F., 2003. BVDV genotypes and biotypes: practical implications for diagnosis and control. Biologicals : journal of the International Association of Biological Standardization 31, 127-131.

Ronecker, S., Zimmer, G., Herrler, G., Greiser-Wilke, I., Grummer, B., 2008. Formation of bovine viral diarrhea virus E1-E2 heterodimers is essential for virus entry and depends on charged residues in the transmembrane domains. The Journal of general virology 89, 2114-2121.
Shen, L., Li, Y., Chen, J., Li, C., Huang, J., Luo, Y., Sun, Y., Li, S., Qiu, H.J., 2014. Generation of a recombinant classical swine fever virus stably expressing the firefly luciferase gene for quantitative antiviral assay. Antiviral research 109, 15-21.
Shoichet, B.K., McGovern, S.L., Wei, B., Irwin, J.J., 2002. Lead discovery using molecular docking. Current opinion in chemical biology 6, 439-446.
Spyrakis, F., Cavasotto, C.N., 2015. Open challenges in structure-based virtual screening: Receptor modeling, target flexibility consideration and active site water molecules description. Archives of biochemistry and biophysics 583, 105-119.
Sun, N., Chan, F.Y., Lu, Y.J., Neves, M.A., Lui, H.K., Wang, Y., Chow, K.Y., Chan, K.F., Yan, S.C., Leung, Y.C., Abagyan, R., Chan, T.H., Wong, K.Y., 2014. Rational design of berberine-based FtsZ inhibitors with broad-spectrum antibacterial activity. PloS one 9, e97514.
Totrov, M., Abagyan, R., 2001. Protein-ligand docking as an energy optimization problem. Wiley, New York.
Wang, Q.Y., Patel, S.J., Vangrevelinghe, E., Xu, H.Y., Rao, R., Jaber, D., Schul, W., Gu, F., Heudi, O., Ma, N.L., Poh, M.K., Phong, W.Y., Keller, T.H., Jacoby, E., Vasudevan, S.G., 2009. A small-molecule dengue virus entry inhibitor. Antimicrobial agents and chemotherapy 53, 1823-1831.
Wang, Z., Nie, Y., Wang, P., Ding, M., Deng, H., 2004. Characterization of classical swine fever virus entry by using pseudotyped viruses: E1 and E2 are sufficient to mediate viral entry. Virology 330, 332-341.
Zhang, Z., Li, Y., Lin, B., Schroeder, M., Huang, B., 2011. Identification of cavities on protein surface using multiple computational approaches for drug binding site prediction. Bioinformatics 27, 2083-2088.

Figure Legends

Figure 1. Identification of a druggable pocket between domains I and II of E2. The protein is represented in ribbon and the ligand binding site in space filling in purple. Domains of E2 are indicated with brackets.

Figure 2. PTC12 inhibits replication of BVDV

A) Cytopathic effect reduction assay for compound PTC12 against BVDV. Antiviral activity of PTC12 against BVDV was performed in MDBK cells. Cells were infected with BVDV (moi 0.01) in the presence of two-fold serial dilutions of compound and incubated for 72 hours. After incubation, cells were fixed and stained with crystal violet, and absorbance at 595 nm was measured in each well. Each dilution was tested at least in triplicates in two individual assays.

B) Antiviral activity of compound PTC12 against BVDV. Data collected from cytopathic effect reduction assay were used to plot log of concentration vs. percentage of inhibition. IC_{50} was estimated from nonlinear regression fitting of the curve.

Figure 3. PTC12 is poorly active against dengue virus 2 (DENV-2, family *Flaviviridae*) and not active against bovine herpesvirus 1 (BHV-1, family *Herpesviridae*).

PTC12 was tested in Vero cells against DENV-2 and in MDBK cells against BHV-1. Cells were infected with DENV-2 or BHV-1 (moi 0.01) in the presence of three dilutions of compound and incubated for 72 hours. Cells were fixed and stained with crystal violet, and absorbance at 595 nm was measured in each well. Each dilution was tested at least in triplicate. Bars represent the mean and standard deviation of the percentage of inhibition in each of the conditions tested.

Figure 4. Design and characterization of a reporter BVDV

A) Schematic representation of cpBVDV/N^{pro} GFP genome. The EGFP coding sequence fused to the 2A autoprotease of foot and mouth disease virus (FMDV) at its 3' terminus was inserted into

the cpBVDV genome between N^{pro} and C. Non strucutral proteins coding sequences are indicated in blue and structural proteins coding sequences in orange.

B) Aminoacidic sequence of the cpBVDV/N^{pro} GFP. The sequence of aminoacids around EGFP-2A insertion is presented. Protein coding sequences are indicated with brackets.

C) GFP correlates with NS3 expression in cpBVDV/N^{pro} GFP infected cells. A representative fluorescence microscopy image acquired with a 40x objective of MDBK cell infected with cpBVDV/N^{pro} GFP. Cells were fixed at 48 hours post infection and stained with a primary αNS3 antibody. Green: GFP; red: NS3; blue: DAPI. Scale bar: 10 µm.

D) Spreading of infection of cpBVDV/N^{pro} GFP. Representative fluorescence microscopy images acquired with 10x objective of MDBK cells infected with cpBVDV/N^{pro} GFP and incubated for 24, 48 or 72 hours. cpBVDV/N^{pro} GFP allows to identify single infected cells at 24 hours post-infection (hpi) and viral foci containing at least 10 infected cells at 48 hpi as. At 72 hpi cytopathic effect of the virus is clearly visible. Green: MDBK-GFP; red: DAPI. Scale bar: 20 µm.

E) Quantification of foci of infection using computer-assisted image analysis. Analysis of a representative image acquired with a 4x objective of cells infected with cpBVDV/N^{pro} GFP and fixed at 48 hpi. (1) Image acquisition: GFP channel corresponding to cpBVDV/N^{pro} GFP infected cells. (2) Threshold setting: thresholding of light objects. (3) Particle analysis: classification of objects according to shape and size, and quantification of foci of infection.

F) Detection of cp-BVDV-GFP infected cells by flow cytometry. MDBK cells were infected with cpBVDV/N^{pro} GFP and the percentage of GFP positive cells was determined by flow cytometry. Histogram of relative fluorescence intensity (FL1) for non-infected cells (control, red line), and

infected cells analyzed at 24 (green line), 48 (blue line) and 72 hpi (orange line). The percentage of positive cells in the gated population is indicated in each plot.

Figure 5. PTC12 inhibits an early step of virus infection

A) Dose-dependent inhibition of cpBVDV/N^{pro} GFP infection with PTC12. MDBK cells were infected with cpBVDV/N^{pro} GFP in the presence of PTC12 at 0.02, 0.4 and 1 µM. Cells were fixed and analyzed by flow cytometry at 48 hpi. The percentages of MDBK-GFP positive cells in each treatment were relativized to non-treated control. Bars represent the mean and standard deviation of the relative percentage of MDBK GFP positive cells from three independent experiments. One way ANOVA with Dunnett post test. *** $P \leq 0.001$.

B) Time of addition assay of compound PTC12. MDBK cells were infected with cpBVDV/N^{pro} GFP and compound was added for 2 hours before infection (pre-addition); at the time of infection (co-addition); or 2, 4 or 6 hours post infection (post-addition). After 24 hpi cells were fixed and analyzed by flow cytometry. The percentages of MDBK-GFP positive cells in each treatment were relativized to non-treated control. Bars represent the mean and standard deviation of the relative percentage of MDBK GFP positive cells from two independent experiments. One way ANOVA with Dunnett post test. * $P \leq 0.05$.

Figure 6. Compound PTC12 is an entry inhibitor of BVDV

A) Addition of compound PTC12 during internalization reduces the number of infection foci. Inhibition of entry by compound PTC12 was tested infecting MDBK cells and adding compound during the attachment or internalization steps. Foci of infection in each treatment were relativized to the number of foci in the untreated control. Bars represent the mean and standard deviation of three independent experiments for the percentage of foci relative to control in each of the conditions tested. One way ANOVA with Dunnett post test. *** $P \leq 0.001$.

B) PTC12 does not affect the yield of attached virus. MDBK cells were infected with cpBVDV/N^{pro} GFP on ice in the presence of PTC12 to allow virus attachment. Attached virus was recovered by cell lysis and was used to infect a new cell monolayer. The percentage of MDBK-GFP positive cells in PTC12 treated cells was relativized to non-treated control. Bars represent the mean and standard deviation of two independent experiments for the percentage of infected cells relative to control. Unpaired t test. Control vs. PTC12, not significant.

C) PTC12 reduces the yield of internalized virus. MDBK cells were infected with cpBVDV/N^{pro} GFP on ice, and after washing of non-attached virus, cells were treated with PTC12 during internalization at 37 ºC, lifted with trypsin and plated onto a new cell monolayer. The percentage of MDBK-GFP positive cells in PTC12 treated cells was relativized to non-treated control. Bars represent the mean and standard deviation of two independent experiments for the percentage of infected cells relative to control. Unpaired t test. Control vs. PTC12, *** P=0.0005.

Figure 7. BI03 is an antiviral candidate emerging from the virtual screen that inhibits virus entry

A) Antiviral activity of compound BI03 against BVDV. Antiviral activity of BI03 against BVDV was performed in MDBK cells. Cells were infected with BVDV (moi 0.01) in the presence of two-fold serial dilutions of compound and incubated for 72 hours. After incubation, cells were fixed and stained with crystal violet, and absorbance at 595 nm was measured in each well. Each dilution was tested at least in triplicates in two individual assays. Data collected from cytopathic effect reduction assay were used to plot log of concentration vs. percentage of inhibition. IC_{50} was estimated from nonlinear regression fitting of the curve.

B) Time of addition assay of compound BI03. MDBK cells were infected with cpBVDV/N^{pro} GFP and compound was added for 2 hours before infection (pre-addition); at the time of infection (co-addition); or 2, 4 or 6 hours post infection (post-addition). After 24 hpi cells were fixed and analyzed by flow cytometry. The percentages of MDBK-GFP positive cells in each treatment

were relativized to non-treated control. Bars represent the mean and standard deviation of the relative percentage of MDBK GFP positive cells from two independent experiments. One way ANOVA with Dunnett post test. ** $P \leq 0.01$.

C) Addition of compound BI03 during internalization reduces the number of infection foci. Inhibition of entry by compound BI03 was tested infecting MDBK cells and adding compound during the attachment or internalization step. Foci in each treatment were relativized to number of foci in control treatment. When compound BI03 was added during the attachment step it didn't show a reduction of the percentage of foci in comparison to control treatment. When compound BI03 was added during the internalization step it showed a significant reduction of the percentage of foci in comparison to control treatment. Bars represent the mean and standard deviation of three independent experiments for the percentage of foci relative to control in each of the conditions tested. One way ANOVA with Dunnett post test. ** $P \leq 0.01$.

D) Compound BI03 does not affect the yield of attached virus. MDBK cells were infected with cpBVDV/N^{pro} GFP on ice in the presence of BI03 to allow virus attachment. Attached virus was recovered by cell lysis and was used to infect a new cell monolayer. The percentage of MDBK-GFP positive cells in BI03 treated cells was relativized to non-treated control. Bars represent the mean and standard deviation of two independent experiments for the percentage of infected cells relative to control. Unpaired t test. Control vs. BI03, not significant.

E) Compound BI03 reduces the yield of internalized virus. MDBK cells were infected with cpBVDV/N^{pro} GFP on ice, and after washing of non-attached virus, cells were treated with BI03 during internalization at 37 ºC, lifted with trypsin and plated onto a new cell monolayer. The percentage of MDBK-GFP positive cells in BI03 treated cells was relativized to non-treated

control. Bars represent the mean and standard deviation of two independent experiments for the percentage of infected cells relative to control. Unpaired t test. Control vs. BI03, * P=0.035.

Figure 8. Predicted interaction of compounds BI03 and PTC12 with E2 extracted from the docking simulation. (A) Ribbon representation of protein E2 with compound BI03 (purple sticks) and PTC12 (orange sticks) within the predicted binding site at the interface between domains I and II. (B and C) 3D Van der Waals molecular surface representations of (B) PTC12 and (C) BI03 in the ligand binding site of E2 from BVDV genotype 1. (D) Representation of PTC12 in the ligand binding site of E2 from BVDV genotype 2. White: neutral surface; green: hydrophobic surface; red: hydrogen bonding acceptor potential; blue: hydrogen bonding donor potential.

Scheme 1. Reagents and conditions. **A)** (a) HCl, H_2O, reflux. **B)** (b) NaOH 2M, methanol, 70 °C, 24 h; (c) $SOCl_2$, NH_3, acetonitrile, r.t; (c) DIPEA, THF, r.t.

Appendix A. Supplementary data. ^{1}H NMR and ^{13}C NMR spectra of representative compounds.

Appendix B. Supplementary Figure 1. (A) Ribbon representation of an homology model of E2 from BVDV genotype 2 with compound PTC12 (sticks) within the predicted binding site at the interface between domains I and II. (B and C) 2D interaction of (B) PTC12 and (C) BI03 in the binding site of protein E2 of BVDV genotype 1. (D) 2D interaction of PTC12 in the binding site of protein E2 of BVDV genotype 2. Pink lines represent hydrogen bonds, π–cation interactions between aromatic rings and Arg residues are shown by solid lines.

Table 1. Antiviral activity of active compounds against BVDV

	CC50 (µM)[1]	IC50 (µM)[2]	
		BVDV type 1a [3]	BVDV type 2 [4]
PTC12	89.520 ± 1.152	0.304 ± 0.131	0.026 ± 0.002
BI03	> 200	17.599 ± 6.427	NT [5]

[1] CC50: cytotoxic concentration 50%. Data represent the mean and standard deviation of at least two independent experiments.

[2] IC50: inhibitory concentration 50%. Data represent the mean and standard deviation of at least two independent experiments.

[3] NADL strain

[4] VS253 strain

[5] NT: not tested.

Figure 1

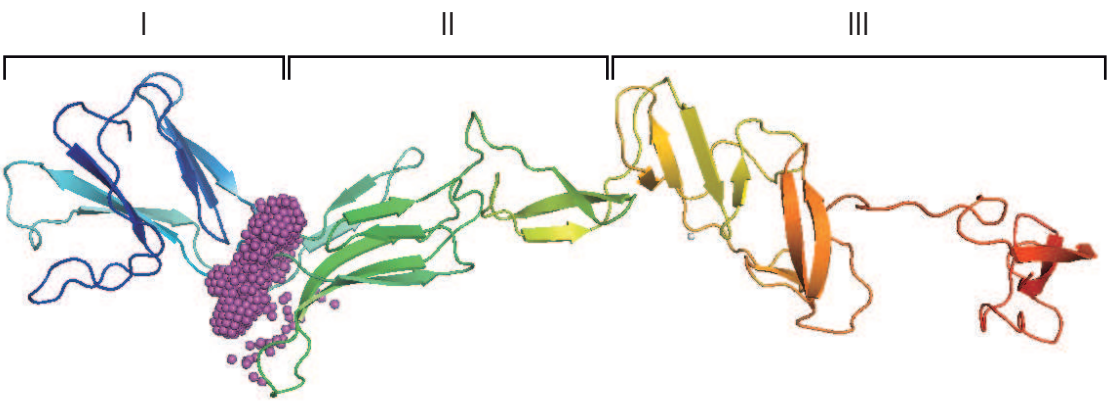

Figure 2

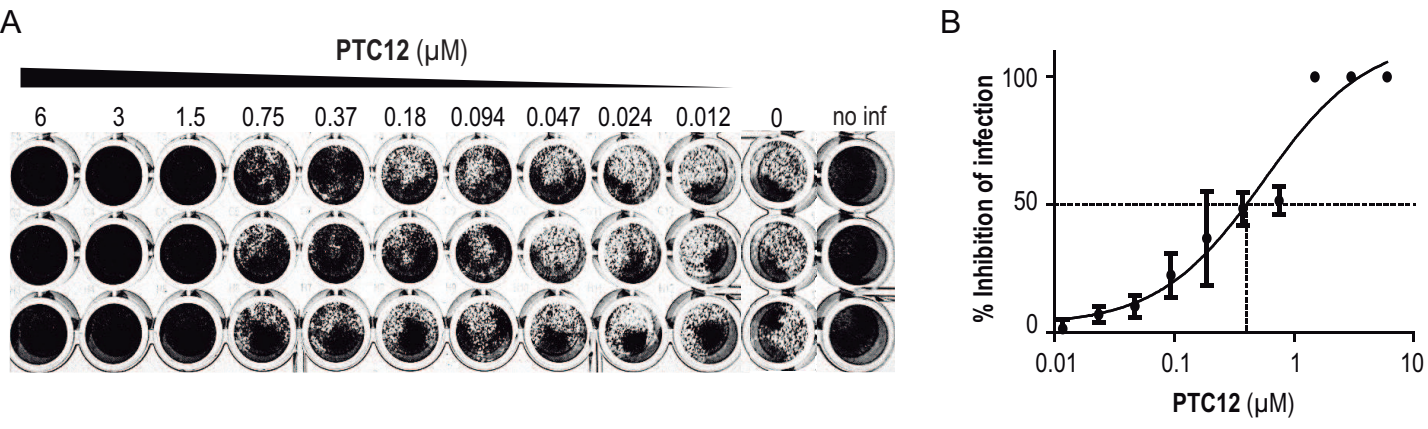

Figure 3

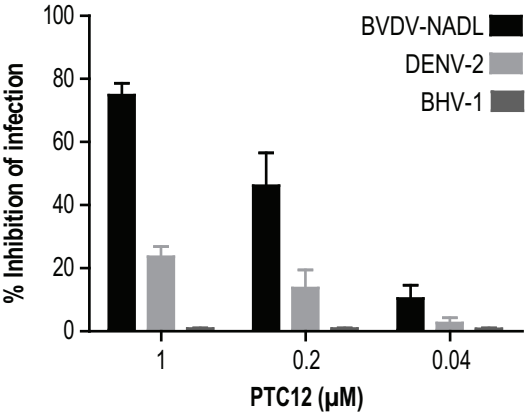

Figure 4

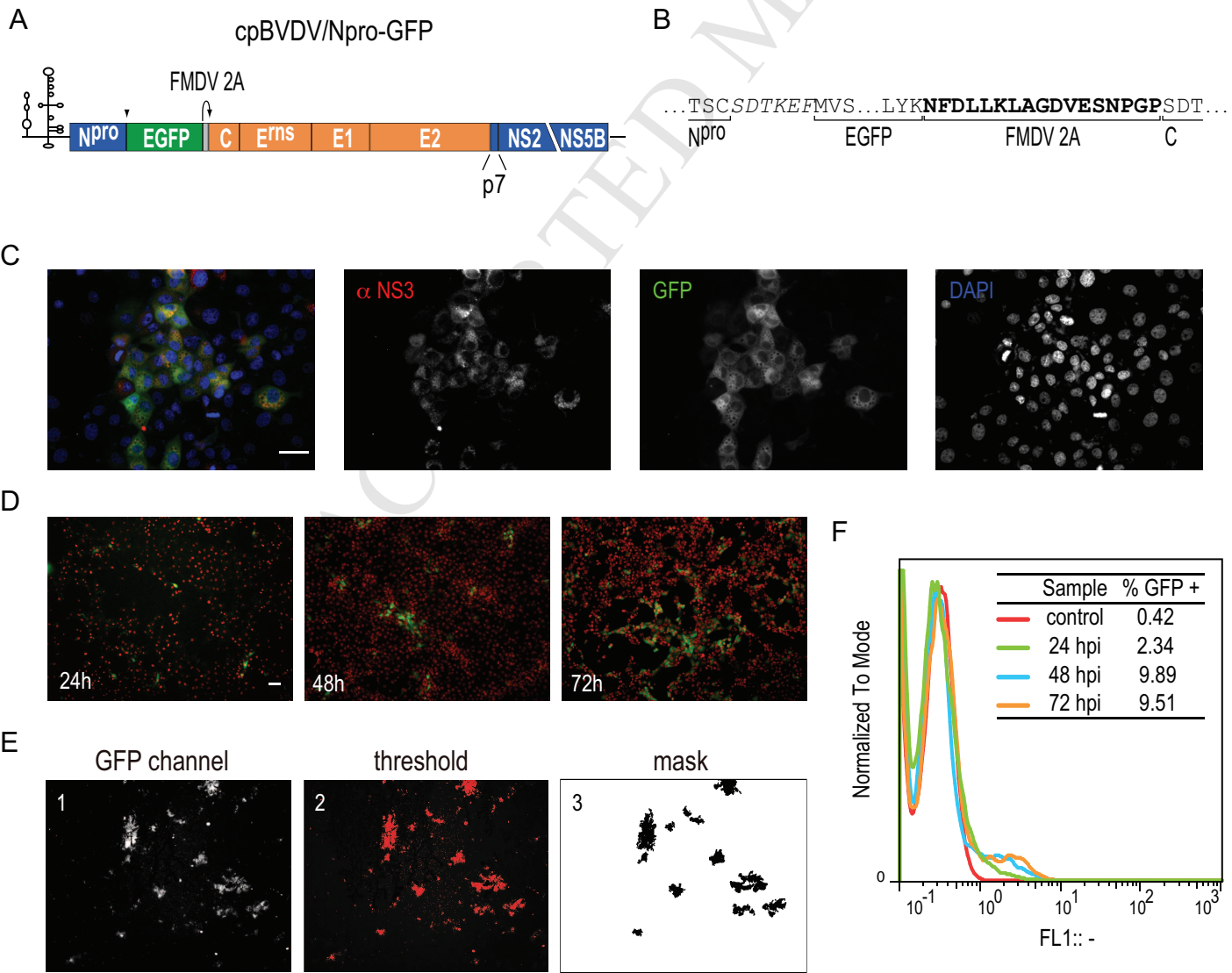

Figure 5

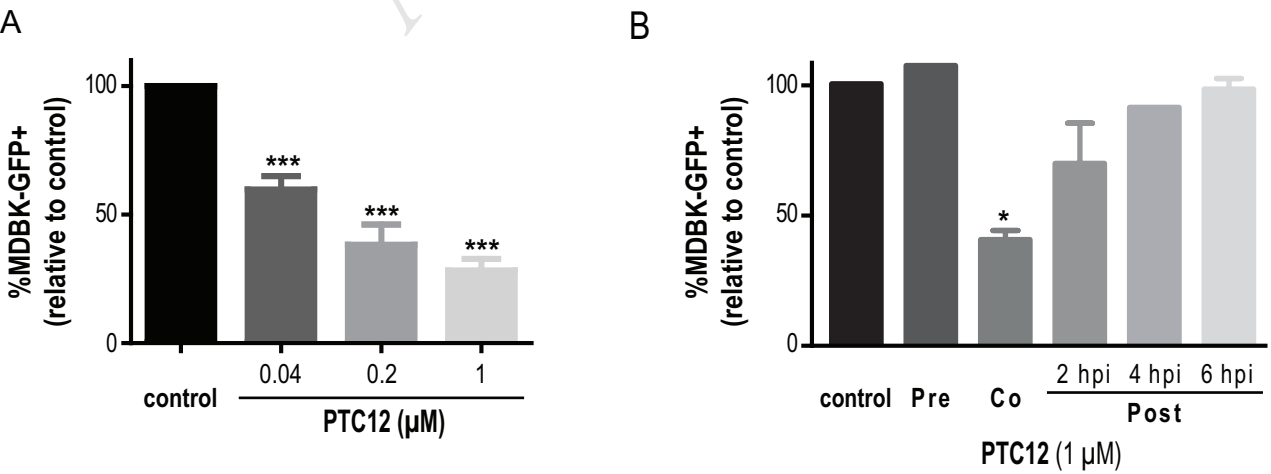

Figure 6

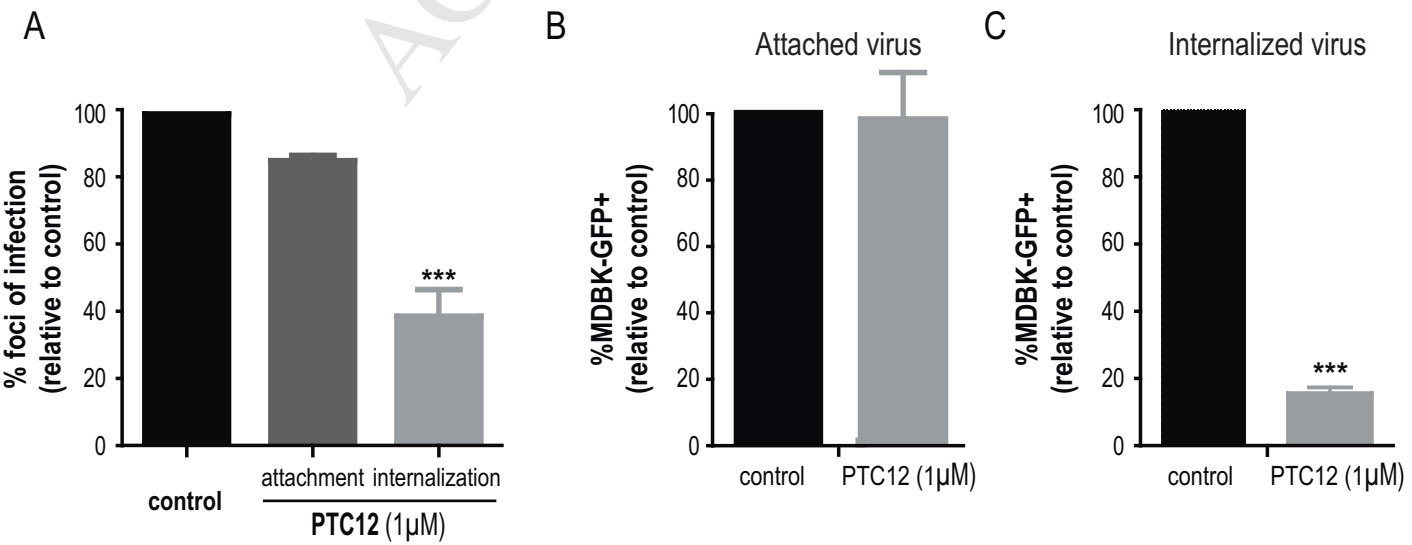

Figure 7

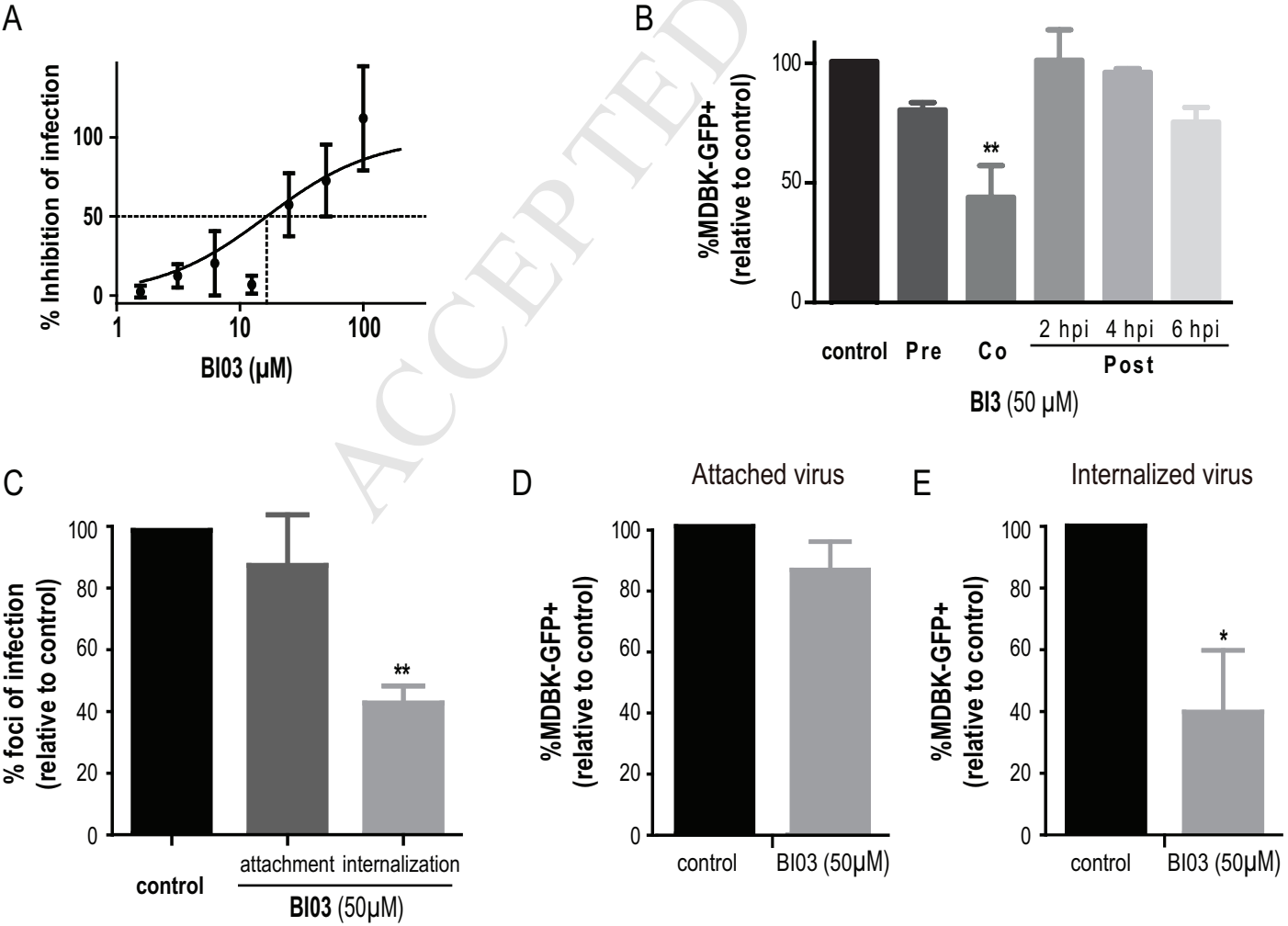

Figure 8

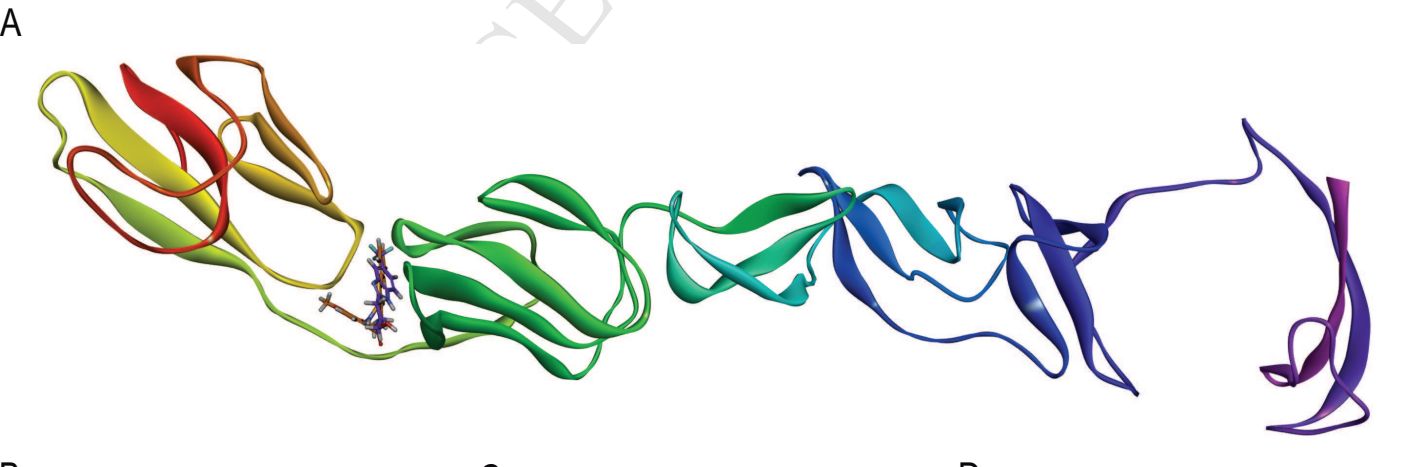

Scheme 1

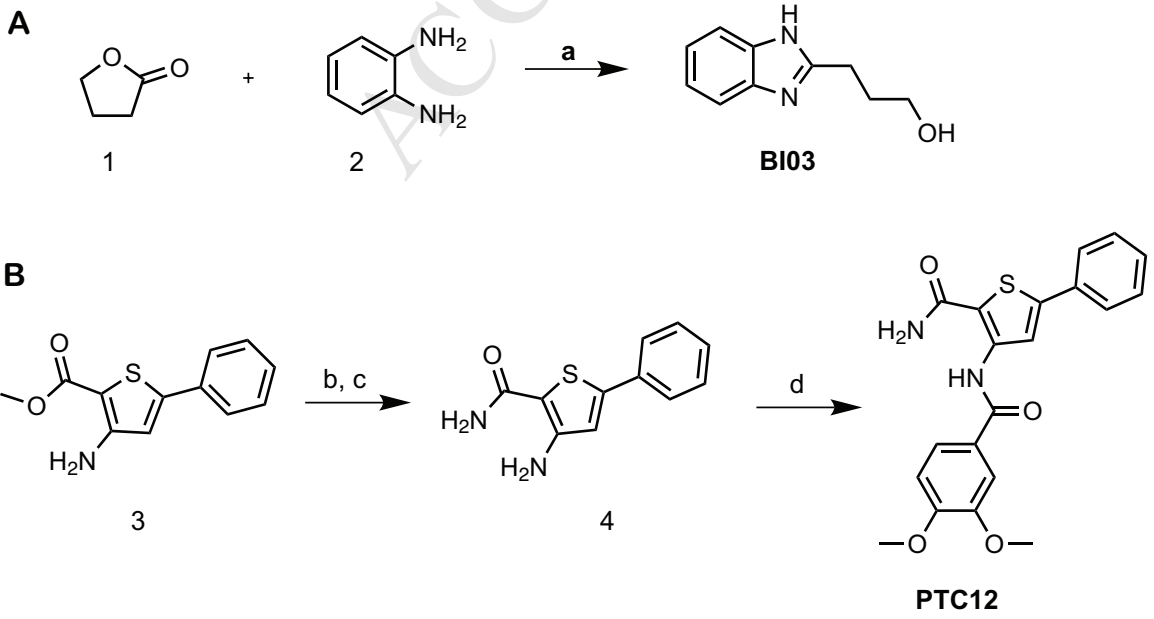

Highlights

“Structure-based drug design for envelope protein E2 uncovers a new class of bovine viral diarrhea inhibitors that block virus entry”

> Docking-based virtual screening was used to develop new antiviral compounds against envelope protein E2 of BVDV
> Candidate compound PTC12 showed antiviral activity in the submicromolar range against BVDV genotype 1a and 2
> A reporter BVDV carrying GFP was designed and used to follow viral infection by flow cytometry and fluorescence microscopy
> Novel molecules emerging from the virtual screening inhibited entry by blocking internalization